Article

Source-Load Collaborative Optimization Method Considering Core Production Constraints of Electrolytic Aluminum Load

Yibo Jiang [1], Zhe Wang [1], Shiqi Bian [2,*], Siyang Liao [2] and Huibin Lu [1]

1   State Grid (Suzhou) City & Energy Research Institute, Suzhou 215000, China; jiangyibo@whu.edu.cn (Y.J.); zwan316@126.com (Z.W.); l1070988313@gmail.com (H.L.)
2   School of Electrical and Automation, Wuhan University, Wuhan 430072, China; liaosiyang@whu.edu.cn
*   Correspondence: bianshiqi@whu.edu.cn; Tel.:+86-13472716286

Abstract: With the deep implementation of the national "dual carbon" strategy, the development of a new power system dominated by renewable energy has accelerated significantly. Electrolytic aluminum load, as an important energy-intensive industrial resource, possesses response flexibility, providing a critical pathway for the efficient utilization of renewable energy. However, ensuring the safety of its production process during demand-side response remains a key challenge. This study systematically investigates the core production constraint of electrolytic aluminum load—electrolytic bath temperature—and its impacts on chemical reaction rates, current efficiency, and production equipment. A detailed coupling relationship between core production constraints and active power regulation is established. By quantifying the effects of temperature variation on the electrolytic aluminum production process, a demand-side response control cost model for electrolytic aluminum load is proposed. Additionally, a day-ahead scheduling model is developed with the objective of minimizing system operating costs while considering the participation of electrolytic aluminum load. Simulation results demonstrate that this method significantly reduces wind curtailment and load shedding while ensuring the safety of electrolytic aluminum production. It provides a novel approach for enhancing system economic efficiency, improving renewable energy utilization, and promoting the deep integration of power systems with industrial loads.

Keywords: electrolytic aluminum load; production constraint; electrolytic bath temperature; cost modeling; source-load coordination

1. Introduction

In recent years, China's proposed strategic goals of "carbon peak and carbon neutrality" [1] have accelerated the rapid development of new energy in the power system [2]. In 2021, China added a wind power installed capacity of 47.57 GW, bringing the cumulative grid-connected wind power capacity to 328 GW [3]. In 2022, this figure further increased to 365 GW [4]. It is expected that by 2035, China's total wind power installed capacity will reach 1107 GW, accounting for 25.33% of the country's total power generation [5]. However, the strong volatility of wind power output poses stricter requirements for the flexibility and regulation capabilities of the power grid. Fully tapping into the regulation potential of high-energy-consuming loads is an effective method to address the instability in the power system caused by large-scale wind power integration.

Currently, there is significant research focused on high-energy-consuming industrial loads that can provide demand response resources. Gerami N et al. [6] proposed an energy consumption modeling method based on the adjustment characteristics of industrial production equipment during cement, aluminum, and steel production, and established an optimization scheduling model for microgrids under a demand response mechanism. Li et al. [7] introduced a load optimization method for high-energy-consuming enterprises based on load transfer scheduling and analyzed the wind power absorption potential and

associated economic benefits in the new energy microgrid of high-energy-consuming enterprises. Liu et al. [8] established a peak load shifting model for electric melting magnesium furnaces based on their working principles, which not only enhanced the flexibility of peak regulation in the power system but also improved wind power absorption capacity. Wu et al. [9] utilized the interruptible load characteristics of industrial users and their willingness to participate in demand response to construct a model based on Gaussian process regression to assess the demand response potential of industrial users. Yang et al. [10] proposed an optimal spatial–temporal pricing strategy for CSs based on the group price response behavior of EVs. Han et al. [11] established an environmental economic dispatch model for a coordinated power system including wind power generation, utilizing a tiered time-of-use pricing approach to encourage cement plants to participate in demand response.

Electrolytic aluminum has a typical high-energy-consumption load with thermal energy storage characteristics. The electrolytic aluminum industry in China plays a pivotal role globally, accounting for 57.18% of the world's output and approximately 7% of the national electricity consumption [12], indicating substantial adjustment potential. However, the premise for electrolytic aluminum manufacturers to participate in demand-side response is that their own safe production can be guaranteed. Chen et al. [13] proposed a multi-time-scale rolling scheduling optimization model that incorporates the demand response characteristics of typical industrial loads, such as electrolytic aluminum, by integrating conditional deep convolutional generative adversarial networks with multi-scenario stochastic programming. Wang et al. [14] established a multi-stage demand response model for electrolytic aluminum loads, exploring the issue of electrolytic aluminum's participation as a flexible resource on the demand side in system regulation. Yue et al. [15] combined electrolytic aluminum with thermal power for deep peak shaving, establishing a hierarchical optimization model for joint peak regulation. Li et al. [16] quantified the regulation capacity of electrolytic aluminum loads and incorporated it into the coordinated optimization scheduling of regional power grids. However, the above literature is relatively lacking in consideration of the production safety and benefits of electrolytic aluminum, and only makes a simple restriction on the adjustment power of electrolytic aluminum load. At present, only a few studies pay attention to the production constraints of electrolytic aluminum. Yue et al. [17] divided the electrolytic cell into three states, production reduction, heat preservation, and cooling, and studied the control cost under different states.

Due to the multiple constraints of the production process of aluminum electrolysis loads, along with characteristics such as nonlinearity, time-variability [18,19], and complex coupling [20,21], establishing models for the electrolytic cells presents significant challenges. In terms of production safety, Guo et al. [22] investigated the power regulation method of electrolytic aluminum under energy balance. Peng et al. [23] indicated that current efficiency is a comprehensive reflection of various economic indicators in the aluminum electrolysis process and serves as an important measure of product yield and quality. It is noted in [24] that temperature is a key factor influencing product yield and quality, establishing a coupling relationship between temperature and current efficiency. Ilyushin et al. [25–27] investigated the five physical fields—electric field, magnetic field, thermal field, flow field, and force field—in aluminum electrolytic cells, deriving higher-order differential equations that describe temperature changes and constructing a comprehensive multiphysics simulation model for aluminum electrolytic cells. Urata K et al. [28] conducted an in-depth analysis of the effects of temperature on equipment lifespan and reliability, proposing a precise method for calculating losses. These studies provide a detailed analysis of the key parameters affecting aluminum electrolysis production from a metallurgical perspective.

In summary, the adjustable characteristics of high-load energy-intensive industrial processes, exemplified by electrolytic aluminum, have attracted widespread attention from scholars both domestically and internationally. However, the production process constraints for electrolytic aluminum are numerous and exhibit nonlinearity and complex coupling. Ensuring that these processes meet key constraints during control is the most crucial

prerequisite for their participation in grid interaction control. It is essential to conduct detailed modeling of the impact of power regulation on core production parameters to ensure that the influence of power support on the production of electrolytic aluminum is minimized. Therefore, this paper first analyzes the effects of electrolytic cell temperature on the reaction rate, current efficiency, and production equipment, establishing a cost model for the demand-side response control of electrolytic aluminum loads that considers the temperature constraints of the electrolytic cell. Next, the process of collaborative day-ahead optimization scheduling between the grid and load is analyzed, and various cost models and operational constraints for both the power supply side and load side within the system are examined. Finally, based on the cost model for controlling electrolytic aluminum loads, a source-load collaborative optimization model is established with the objective function of minimizing the sum of various costs, considering the participation of electrolytic aluminum loads.

2. Aluminum Electrolytic Load Control Cost Model Based on Temperature Constraints

2.1. The Impact of Cell Temperature on Production

Temperature is an important indicator of the thermal equilibrium state within a cell. The impact of temperature changes caused by electrolytic aluminum loads during the control process on production is a complex process, primarily reflected in its effects on the reaction rate, current efficiency, and production equipment.

(1) The Effect of Temperature on Reaction Rate

The rated temperature for aluminum electrolysis load production is 960 °C. When the temperature limits are between 950 °C and 970 °C, according to the van't Hoff approximation, the reaction rate increases approximately 2 to 4 times for every 10 °C rise in temperature. This rule can be used to roughly estimate the effect of temperature variations on the reaction rate. Therefore, within the range of [950 °C, 970 °C], this paper expresses the coupling relationship between temperature and the reaction rate of aluminum electrolysis load using Equation (1).

$$v(T) = v(T_N)\lambda^{(T-T_N)/10} \tag{1}$$

where $v(T)$ represents the electrolysis reaction rate at temperature $T°C$, and $v(T_N)$ represents the electrolysis reaction rate at the rated temperature $T_N°C$. According to the approximation, the range of λ is from 2 to 4.

(2) The Effect of Temperature on Current Efficiency

Current efficiency refers to the ratio of electric current converted into useful products during an electrochemical reaction, reflecting the energy utilization efficiency and economic viability of the reaction system; it is a crucial indicator. In electrochemical reactions, only a portion of the electric current is used to produce useful chemical substances, while other portions are lost in various forms, such as heat, light, and gasses. These losses lead to energy waste in the reaction system. In modern electrolytic cells, it is generally believed that for every 10 °C decrease in electrolytic temperature, the current efficiency increases by 1% to 1.5% [24]. The effect of temperature on current efficiency during the molten salt electrolysis of alumina in cryolite is shown in Figure 1.

The curves labeled 1, 2, 3, and 4 in the figure represent the relationships between temperature and current efficiency as determined experimentally by Szeker, Fellner, Vasilev, and Schmitt [24].
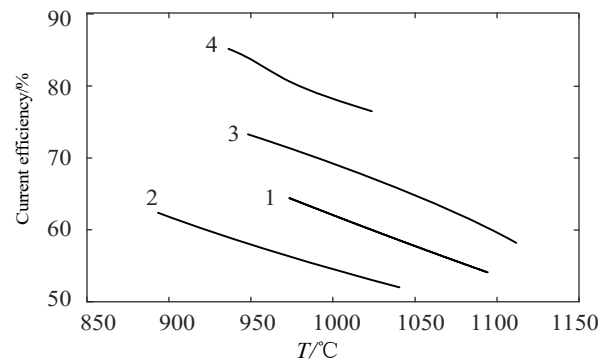
Figure 1. Current efficiency versus temperature during cryolite–alumina molten salt electrolysis.

Based on the curve representing the relationship between current efficiency and temperature, the coupling relationship between current efficiency and electrolytic cell temperature can be expressed as follows:

$$\eta(T) = \eta(T_N) + \rho(T - T_N) \tag{2}$$

where denotes the heat dissipated from the cell system to the surroundings $\eta(T)$ represents the current efficiency at $T°C$; $\eta(T_N)$ denotes the current efficiency at the rated temperature $T_N°C$; ρ is the proportionality coefficient, which varies between -0.15% and -0.10% based on the observed trend.

(3)   The Impact of Temperature on Production Equipment

During the production process of electrolytic aluminum, an increase in temperature can cause thermal expansion of the metal materials within the equipment, potentially leading to deformation, vibrations, and noise issues. Additionally, elevated temperatures can accelerate internal corrosion and metal fatigue within the equipment, both of which contribute to a shortened equipment lifespan. Therefore, while increasing the temperature to enhance the reaction rate, it is also essential to consider the reliability and lifespan of the production equipment and to implement necessary measures to ensure the safe and stable operation of the equipment.

Conversely, if the temperature is too low, the viscosity of the electrolyte will increase, subsequently raising the dynamic pressure of the electrolyte and resulting in a decline in the flow performance within the equipment. Moreover, lower temperatures may also trigger instability in crystallization or sediment within the equipment, which could negatively impact the normal operation and maintenance of the equipment.

Thus, in the production process of electrolytic aluminum, it is crucial to regulate the temperature appropriately to enable the equipment to operate efficiently within a stable working temperature range. At the same time, reasonable maintenance of the equipment is necessary to ensure its lifespan and safety.

2.2. Load Control Cost of Electrolytic Aluminum Considering Cell Temperature Constraints

The economic loss incurred by adjusting the power of electrolytic aluminum load in grid regulation is defined as its control cost. The following will provide a detailed analysis of this control cost. Based on the analysis of the impact of temperature on reaction rate, current efficiency, and production equipment during the regulation of electrolytic aluminum load in Section 2.1, the control cost can be divided into the following three components:

(1)   Change in control cost of electrolytic aluminum load C_v due to changes in the chemical reaction rate:

Since the faster the reaction rate, the higher the output of the electrolytic aluminum load per unit time, the greater the benefit of the electrolytic aluminum load per unit time.

From Equation (1), it can be obtained that the unit time benefit of the electrolytic aluminum load affected by the chemical reaction rate at $T°C$ is $C_{T,v}$.

$$C_N = \alpha M$$
$$C_{T,v} = C_N \lambda^{(T-T_N)/10} \tag{3}$$

Then, the change in electrolytic aluminum load control cost C_v caused by the change in chemical reaction rate can be expressed by the difference between C_N and $C_{T,v}$.

$$C_v = C_N - C_N \lambda^{(T-T_N)/10} \tag{4}$$

where C_N represents the revenue of the electrolytic aluminum load per unit time at the rated temperature; $C_{T,v}$ is the unit time benefit of the electrolytic aluminum load affected by the chemical reaction rate at $T°C$; α is the profit obtained from producing one ton of aluminum; M is the aluminum output per unit time.

(2)　Change in control cost of electrolytic aluminum load C_η due to variations in current efficiency:

According to Equation (2), this paper considers that the unit time benefit of electrolytic aluminum load affected by current efficiency at $T°C$ is $C_{T,\eta}$.

$$C_{T,\eta} = C_N(\eta(T_N) + \rho(T - T_N)) \tag{5}$$

Then, the change C_η in the electrolytic aluminum load control cost caused by the change in current efficiency can be expressed by the difference between C_N and $C_{T,\eta}$.

$$C_\eta = \rho C_N(T - T_N) \tag{6}$$

where ρ is the proportionality coefficient, which varies between -0.15% and -0.10% based on the observed trend.

(3)　Penalty cost CP [29]:

The greater the deviation of the electrolytic cell from the rated temperature, the more significant the impact on the equipment, leading to decreased product yield and quality. Consequently, the penalty cost also increases; thus, the penalty cost for the electrolytic aluminum load can be expressed as follows:

$$C_P = \beta_P \left(\frac{T - T_N}{T_{\max} - T_{\min}}\right)^2 \tag{7}$$

where β_p represents the penalty cost coefficient; $T_{\max}$ and $T_{\min}$ represent the equipment's permissible temperature range.

In summary, the control costs incurred due to temperature changes during the participation of electrolytic aluminum load in demand-side response can be described as follows:

$$C_{Al} = C_v + C_\eta + C_P \tag{8}$$

where C_{Al} represents the total cost associated with the regulation of the electrolytic aluminum load.

2.3. Energy Conversion Analysis of Electrolytic Cells

In the aluminum production process, the energy conversion in the electrolytic cell is primarily manifested as follows.

Energy required for the reaction: During this process, a portion of the electrical energy is converted into thermal energy, raising the temperature within the electrolytic cell to ensure the normal progression of the reaction. Another portion of the electrical energy is converted into chemical energy, which is used to reduce alumina to aluminum metal.

Energy loss: During the aluminum electrolysis process, due to factors such as the conductivity of the electrolyte and losses in the electrolytic cell, electrical energy often cannot be fully converted into the energy required for the chemical reaction, resulting in some energy loss.

In summary, the energy changes in the aluminum electrolytic cell are primarily characterized by the conversion of electrical energy into thermal energy, the conversion of electrical energy into chemical energy, and energy losses. The energy conversion process within the electrolytic cell can be represented by Equation (9):

$$E_{input} = E_{reaction} + E_{loss} \tag{9}$$

$$E_{input} = P_{Al}t \tag{10}$$

where E_{input} represents the energy input into the electrolytic cell; $E_{reaction}$ is the energy required by the reaction system; E_{loss} denotes the heat dissipated from the cell system to the surroundings; P_{Al} is the input power of the electrolytic cell; and t is the time.

When the active power input of the electrolytic aluminum load changes, it primarily causes temperature variations in the electrolytic cell. Utilizing the specific heat capacity formula, a conversion relationship can be established between the core production indicator—production temperature—and the load adjustment amount ΔP_{Al}, as shown in Equation (11):

$$(P_t^{Al} - P_{t-1}^{Al})\Delta t = cm(T_t - T_{t-1})$$
$$\Downarrow \tag{11}$$
$$\Delta P_{Al}\Delta t = cm\Delta T$$

where P_t^{Al} and P_{t-1}^{Al} represent the input power of the electrolytic cell at times t and $t-1$, respectively, while T_t and T_{t-1} represent the corresponding temperatures. c denotes the specific heat capacity of the molten electrolyte, and m is the mass of the molten electrolyte.

Combining Equations (8) and (11), the coupling relationship between the control cost arising from temperature changes and the active adjustment amount is given by the following:

$$C_T = -C_N\sigma^{a_T(\Delta P_{Al}\Delta t)+b_T} + p_T(\Delta P_{Al}\Delta t)^2$$
$$+q_T(\Delta P_{Al}\Delta t) + h_T \tag{12}$$

where a_T, b_T, p_T, q_T, and h_T are the cost coefficients that account for the effects of power regulation.

$$a_T = \frac{1}{10cm}; b_T = \frac{T-T_N}{10};$$
$$p_T = \frac{\beta_p}{(cm(T_{max}-T_{min}))^2};$$
$$q_T = \frac{\lambda C_N}{cm} + 2\beta_p\frac{T-T_N}{(T_{max}-T_{min})^2}; \tag{13}$$
$$h_T = C_N + \lambda C_N(T - T_N) + \beta_p\frac{(T-T_N)^2}{(T_{max}-T_{min})^2}$$

The Figure 2 shows the change curve of the coupling between the electrolytic aluminum load control cost and the electrolytic cell temperature under different adjustment amounts (ΔP_{Al}). The change in control cost is mainly determined by the influence of the electrolytic cell temperature on the reaction rate, current efficiency, and equipment performance of the production process, as follows.
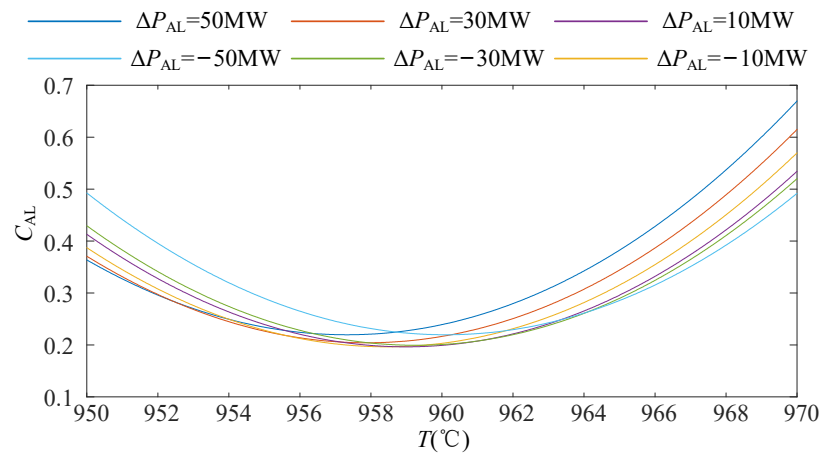
Figure 2. Costs of aluminum load control under different regulation scenarios.

When the temperature is around 960 °C, the control cost of the electrolytic aluminum load is the lowest. This is because this temperature is close to the rated process temperature of electrolytic aluminum production, which can maximize the stability of the production process and the life of the equipment. In this range, the reaction rate, current efficiency, and equipment burden are all within a reasonable range.

When the load is adjusted upward, the increase in ΔP_{Al} will cause the temperature of the electrolytic cell to gradually increase. According to model Formula (11), the increase in temperature accelerates the reaction rate, but at the same time may cause a decrease in current efficiency and the risk of equipment overload. This temperature deviation increases the uncertainty of production and ultimately increases the load control cost. Especially when ΔP_{Al} increases significantly, the temperature rises more significantly, and the impact on equipment life and safe operation is more significant.

When the load is adjusted downward, the decrease in ΔP_{Al} causes the electrolytic cell temperature to gradually decrease. If the temperature deviates from the rated value (below 950 °C), it may cause the electrolytic cell to become cold, significantly reducing the reaction rate and current efficiency, while increasing equipment energy loss and operating risks. Therefore, as ΔP_{Al} further decreases, the load control cost shows an increasing trend.

3. Day-Ahead Economic Dispatch Optimization Model Considering Electrolytic Aluminum Load

3.1. Objective Function

For the day-ahead scheduling, an optimal configuration of generation and load resources is comprehensively considered. The generation side includes thermal power units and wind power, while the load side takes into account the role of aluminum electrolysis in regulating peak and valley loads in the power grid. The objective is to minimize the total operating costs of the system, and the formulation of the objective function is detailed as follows:

$$\min C = C_1 + C_2 + C_3 + C_4 + C_5 + C_{Al} \tag{14}$$

$$C_1 = \sum_{i=1}^{n} \sum_{t=1}^{T} u_{i,t}\left(x_i \left(P_{i,t}^{th}\right)^2 + y_i P_{i,t}^{th} + z_i\right) \tag{15}$$

$$C_2 = \sum_{i=1}^{n} \sum_{t=1}^{T} \left(u_{i,t}(1 - u_{i,t-1})c_{i,t}^u + u_{i,t-1}(1 - u_{i,t})c_{i,t}^d\right) \tag{16}$$

$$C_3 = \sum_{i=1}^{n} \sum_{t=1}^{T} \left(c_i^{up} R_{i,t}^{up} + c_i^{dn} R_{i,t}^{dn}\right) \tag{17}$$

$$C_4 = \sum_{j=1}^{w} \sum_{t=1}^{T} \left(c_{wind} \left(P_{j,t}^{wf} - P_{j,t}^{w} \right) \right) \tag{18}$$

$$C_4 = \sum_{j=1}^{w} \sum_{t=1}^{T} \left(c_{wind} \left(P_{j,t}^{wf} - P_{j,t}^{w} \right) \right) \tag{19}$$

where C represents the total cost of the system; C_1 denotes the fuel cost of the thermal power unit; C_2 indicates the startup and shutdown costs of the thermal power unit; C_3 refers to the standby cost of the thermal power unit; C_4 represents the cost of curtailment due to wind power; and C_5 denotes the load shedding cost of the system; n is the number of thermal power units participating in the scheduling; T is the total time period of the scheduling cycle; $u_{i,t}$ is a binary variable indicating whether thermal power unit i is operational during time period t, $P_{i,t}^{th}$ represents the output power of thermal power unit i during time period t; x_i, y_i, and z_i are coefficients related to fuel costs; $c_{i,t}^{u}$ represents the cost coefficients for the startup of thermal power unit i during time period t; $c_{i,t}^{d}$ denotes the cost coefficient for the shutdown of thermal power unit i; c_i^{up} and c_i^{dn} represent the cost coefficients for the upward and downward reserve services provided by thermal power unit i, respectively; $R_{i,t}^{up}$ and $R_{i,t}^{dn}$ represent the upward and downward reserve capacities provided by thermal power unit i during time period t; w is the total number of wind power units; c_{wind} is the penalty cost coefficient incurred due to the underutilization of wind power. $P_{j,t}^{wf}$ represents the forecasted generation of wind power unit j during time period t; $P_{j,t}^{w}$ denotes the actual generation of wind power unit j during time period t; c_{load} is the cost coefficient for load reduction. P_t^{loadf} is the forecasted load value for time period t; P_t^{load} denotes the actual load value for time period t.

3.2. Constraints

In the day-ahead optimization scheduling process of the system, it is necessary to comprehensively consider various constraint conditions. These constraints include the basic operational requirements of the system, operational limits of thermal power units, the volatility of wind power output, and the production safety constraints of aluminum electrolysis loads. These factors collectively affect the scheduling effectiveness of the system, ensuring that the system meets demand while maintaining the economic and stable operation of the power grid.

3.2.1. Constraints on the Power Supply Side

(1)   System Power Balance Constraint:

$$\sum_{i=1}^{n} P_{i,t}^{th} + \sum_{j=1}^{w} P_{j,t}^{w} = P_t^{load} + P_t^{Al} \tag{20}$$

(2)   Output and Ramp Rate Constraints of Thermal Power Units:

$$u_{i,t} P_{i,\min}^{th} \leq P_{i,t}^{th} \leq u_{i,t} P_{i,\max}^{th} \tag{21}$$

where $P_{i,\min}^{th}$ and $P_{i,\max}^{th}$ denote the minimum and maximum output power allowed for thermal power unit i; $V_{U,i}$ and $V_{D,i}$ represent the rate limits for increasing or decreasing output for thermal power unit i; $S_{U,i}$ and $S_{D,i}$ indicate the rate limits during the startup and shutdown processes of thermal power unit i.

$$\begin{cases} P_{i,t-1}^{th} - P_{i,t}^{th} \leq V_{D,i} u_{i,t} + S_{D,i} (u_{i,t-1} - u_{i,t}) + P_{i,\max}^{th} (1 - u_{i,t-1}) \\ P_{i,t}^{th} - P_{i,t-1}^{th} \leq V_{U,i} u_{i,t-1} + S_{U,i} (u_{i,t} - u_{i,t-1}) + P_{i,\max}^{th} (1 - u_{i,t}) \end{cases} \tag{22}$$

(3)　Minimum Startup and Shutdown Time Constraint:

$$\begin{cases} (T_{i,t-1}^{on} - T_{i,\min}^{on})(u_{i,t-1} - u_{i,t}) \geq 0 \\ (T_{i,t-1}^{off} - T_{i,\min}^{off})(u_{i,t} - u_{i,t-1}) \geq 0 \end{cases} \tag{23}$$

where $T_{i,t}^{on}$ and $T_{i,t}^{off}$ denote the continuous startup and shutdown times of thermal power unit i during time period t; $T_{i,\min}^{on}$ and $T_{i,\min}^{off}$ represent the minimum startup and shutdown times for thermal power unit i.

(4)　Startup and Shutdown Cost Constraints:

$$\begin{cases} C_{i,t}^{U} \geq S_i^{U}(u_{i,t} - u_{i,t-1}) \\ C_{i,t}^{U} \geq 0 \end{cases} \tag{24}$$

$$\begin{cases} C_{i,t}^{D} \geq S_i^{D}(u_{i,t-1} - u_{i,t}) \\ C_{i,t}^{D} \geq 0 \end{cases} \tag{25}$$

where $C_{i,t}^{U}$ represents the start-up cost of unit i during time period t, and $C_{i,t}^{D}$ represents the shut-down cost of unit i during time period t.

(5)　Reserve Constraints:

$$\begin{cases} 0 \leq R_{i,t}^{up} \leq \min(u_{i,t}P_{i,\max}^{th} - P_{i,t}^{th}, V_{U,i}) \\ 0 \leq R_{i,t}^{dn} \leq \min(P_{i,t}^{th} - u_{i,t}P_{i,\min}^{th}, V_{D,i}) \end{cases} \tag{26}$$

(6)　Wind Power Output Constraints:

$$0 \leq P_{j,t}^{w} \leq P_{j,\max}^{wf} \tag{27}$$

where $P_{j,\max}^{wf}$ represents the predicted maximum output of wind turbine j during time period t.

3.2.2. Constraints on the Load Side

The production process of aluminum electrolysis involves using molten aluminum as the cathode and carbon materials as the anode, along with molten cryolite as a solvent. When a large direct current passes through the electrolytic cell, it generates substantial heat, maintaining the cell temperature between 950 °C and 970 °C, thereby ensuring that the electrochemical reactions at both electrodes proceed normally [30].

When adjusting the load for aluminum electrolysis, the following key constraints must be considered.

(1)　Load Power Constraints:

$$P_t^{Al} = P_{rated}^{Al} + \Delta P_t^{Al} \tag{28}$$

$$\Delta P_{\min}^{Al} \leq \Delta P_t^{Al} \leq \Delta P_{\max}^{Al} \tag{29}$$

where P_{rated}^{Al} represents the rated power of aluminum electrolysis load, while $\Delta P_{\min}^{Al}$ and $\Delta P_{\max}^{Al}$ denote the minimum and maximum values of the power adjustment for the aluminum electrolysis load, respectively.

(2)　Electrolyzer Temperature Constraints:

$$T_{\min} \leq T_t \leq T_{\max} \tag{30}$$

where T_t represents the temperature of the electrolytic cell during time period t; $T_{\min}$ and $T_{\max}$ denote the minimum and maximum temperature values that satisfy the production conditions of the electrolytic cell, respectively.

(3)   Power Regulation Constraints:

$$\Delta P^{Al}_{\min} = (T_{\min} - T(t))cm/\Delta t \tag{31}$$

$$\Delta P^{Al}_{\max} = (T_{\max} - T(t))cm/\Delta t \tag{32}$$

(4)   Conventional Load Constraints:

$$0 \leq P^{load}_t \leq P^{loadf}_t \tag{33}$$

4. Case Study Analysis

4.1. Case Study Parameter Settings

This paper conducts a simulation and in-depth analysis of the improved IEEE-30 node system, as shown in Figure 3. The improved system includes six conventional thermal power units G1-G6 and a wind farm with an installed capacity of 1500 MW; the parameters of the thermal power units are shown in Table 1, while the rated capacity of the aluminum electrolysis load is 400 MW. The scheduling period is 24 h, with scheduling occurring once every hour. The model proposed in this paper is solved using the CPLEX solver in MATLAB R2021a.
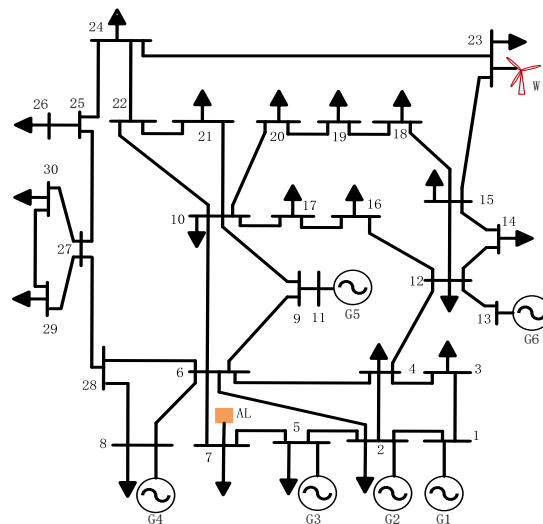

Figure 3. Improved IEEE-30 node system.

Table 1. Selected operating parameters of thermal power units.

Unit	Pmin/MW	Pmax/MW	a/(yuan/MW h^2)	b/(yuan/MW h)	c/(yuan/h)
G1	195	390	0.108	50.57	1240.437
G2	75	150	0.105	56.07	1607.977
G3	125	250	0.096	50.05	1320.285
G4	100	200	0.223	63.94	1680.321
G5	50	100	0.118	68.86	2480.693
G6	50	100	0.153	69.86	2120.3478

As illustrated in the wind power forecast curve in Figure 4, significant peaks in wind power output are observed from 2:00 A.M. to 6:00 A.M. and from 5:00 P.M. to 8:00 P.M.
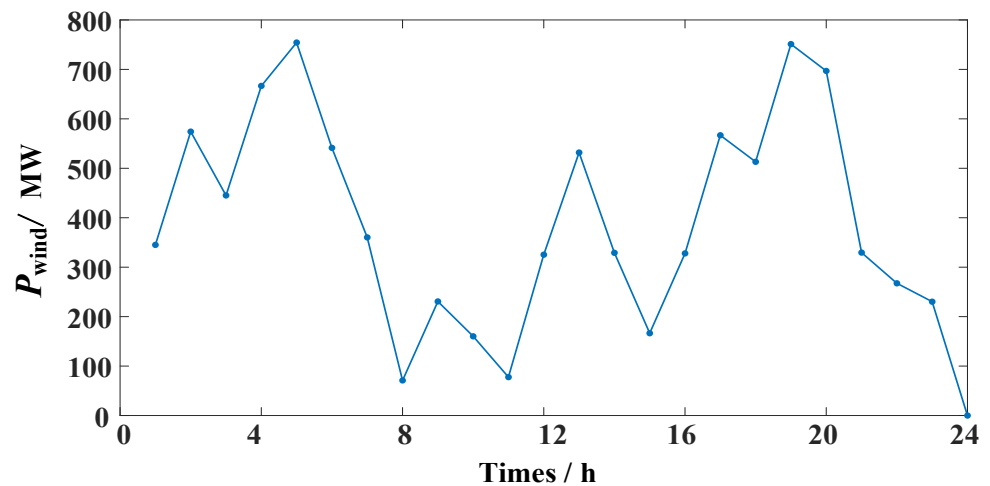
Figure 4. Forecast curve of wind power generation.

However, during these periods, the conventional load demand in Figure 5 is at a low point, resulting in a relatively low utilization efficiency of wind power within the system. In contrast, during the peak periods of conventional load, wind power output significantly decreases, reaching a low state. This phenomenon exhibits a clear "reverse peak shaving" characteristic between wind power and conventional load, complicating the regulation of thermal power units. This leads to severe issues of curtailment and load shedding, which not only increase the scheduling costs of the system but also result in energy waste. Therefore, there is a need to further optimize the utilization of wind power resources to enhance their economic efficiency and reliability.
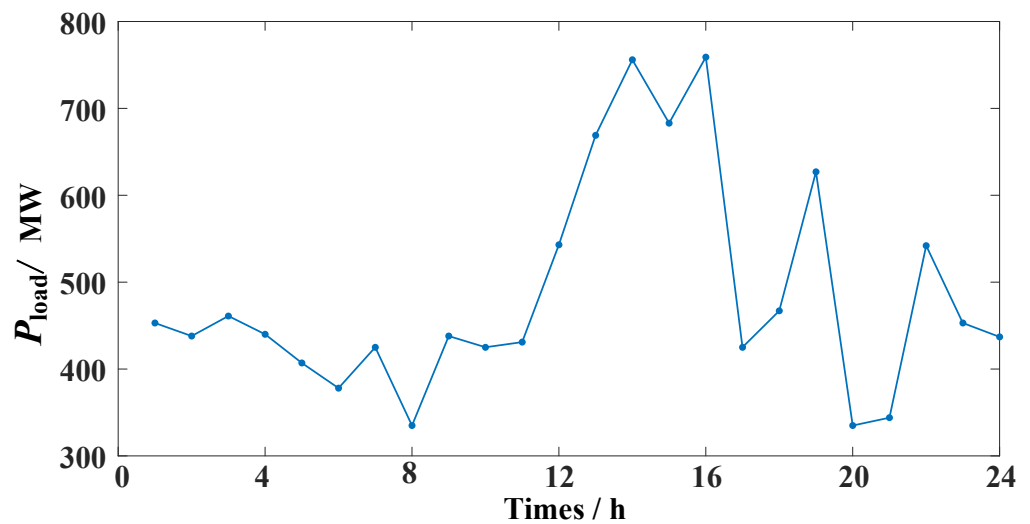

Figure 5. Conventional load forecast power curve.

4.2. Scenario Setup

To thoroughly analyze the impact of electrolytic aluminum loads on day-ahead optimal dispatch, this study defines two scenarios for comparative analysis.

Scenario 1: Only thermal power units participate in the peak shaving of the grid. By analyzing Scenario One, this study examines the impact on the day-ahead optimal dispatch of the power system when no electrolytic aluminum load provides ancillary services.

Scenario 2: The electrolytic aluminum load collaborates with thermal power units to perform grid peak shaving. In this scenario, the study investigates the overall impact of the electrolytic aluminum load providing ancillary services on the day-ahead optimal dispatch

of the power system, further exploring its effect on improving system operational efficiency and economic benefits.

4.3. Analysis of Case Study Results

4.3.1. Analysis of System Operating Costs

By comparing the costs in both scenarios, it can be seen from the results in Table 2 that while Scenario Two increases the adjustment costs of the electrolytic aluminum load, the fuel costs, load shedding costs, and curtailment costs of the units are all lower than those in Scenario One. Therefore, the total operating cost of the grid in Scenario Two is less than that in Scenario One. The adjustment model proposed in this paper, which considers the participation of electrolytic aluminum loads, can enhance the operational economy of the power grid.

Table 2. Comparison of system operating costs in different scenarios.

Cost	Scenario 1	Scenario 2
Total operating cost of the power grid/yuan	3.6231×10^6	3.4549×10^6
Fuel cost of the unit/yuan	7.5730×10^5	7.5690×10^5
Load shedding cost/yuan	5.3860×10^4	3.9363×10^4
Curtailed wind cost/yuan	2.7741×10^6	2.4320×10^6
Adjustment cost of electrolytic aluminum/yuan	/	1.8872×10^5

4.3.2. Analysis of Wind Power Utilization and Load Shedding

The output of wind power and the comparison of load shedding power in both scenarios are shown in Figures 6 and 7. According to the MAE statistical indicator, the average absolute error between wind power output and load power in Scenario 2 is smaller compared to Scenario 1.During the period from 1:00 to 6:00, the planned output of wind power is lower than the predicted wind power, while the load power remains at a low level during the same period. Due to the limited downward adjustment capacity of thermal power units, the curtailment of wind power during this period is quite severe.
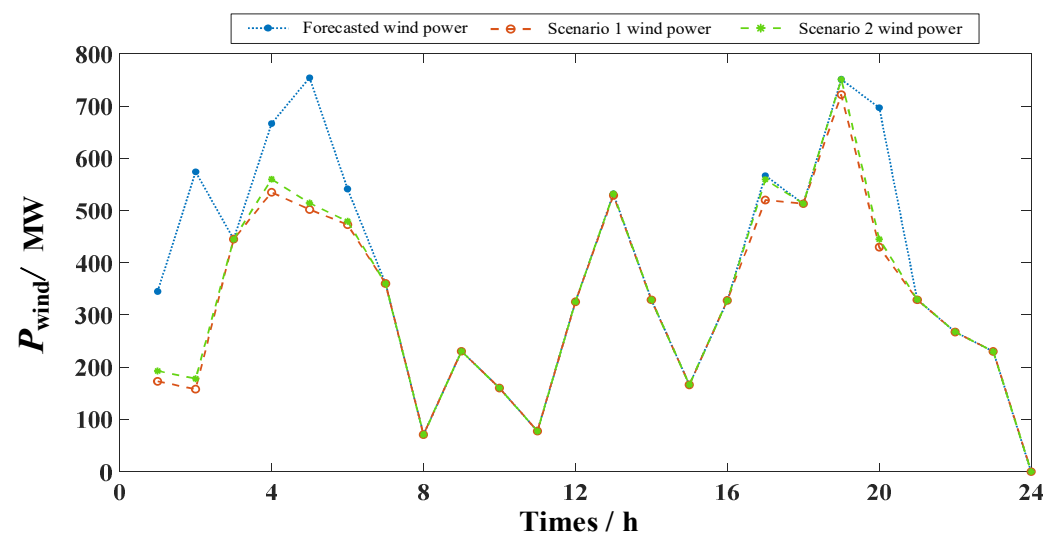

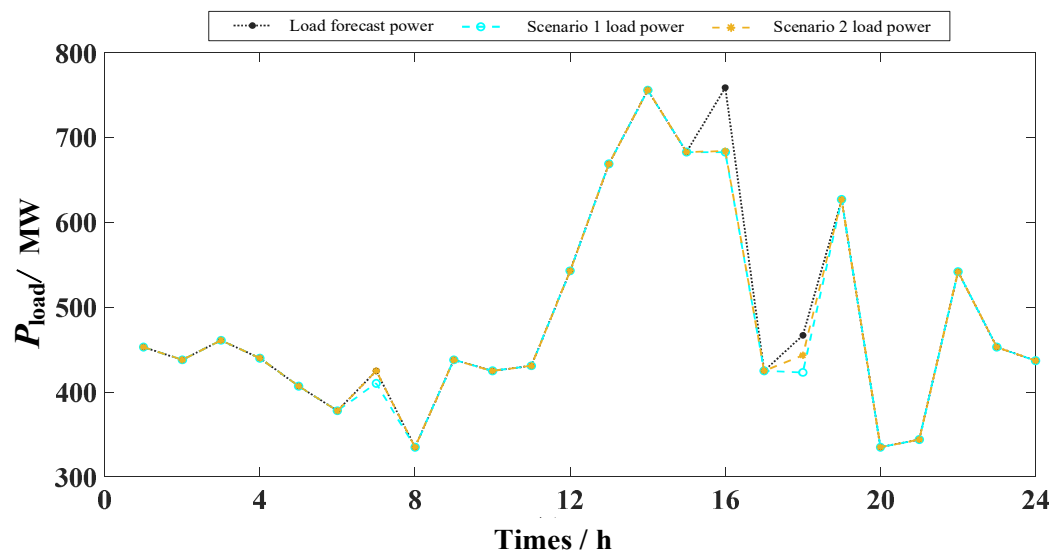**Figure 6.** Comparative chart of actual wind power output.

Figure 7. Comparative chart of regular load power.

As shown in Figure 6, over the course of 24 h periods in a day, Scenario One experiences restrictions on the output of wind power during 8 time periods due to the lack of consideration for electrolytic aluminum load participation in peak-shaving. The total absorbed wind power is 7.8757×10^3 MW, with a curtailment rate of 14.97%. In Scenario Two, after considering the participation of electrolytic aluminum loads in peak-shaving, wind power output is restricted during 7 time periods, with a total absorbed wind power of 8.0468×10^3 MW and a curtailment rate of 13.13%.

From Figure 7, it can be observed that the system experiences peak electricity consumption during the periods of 10:00 to 14:00 and 18:00 to 21:00. During these times, the output of wind power is relatively low. Due to the limited upward adjustment capacity of thermal power units, it is necessary to shed some load during the periods of 16:00 and 18:00 to maintain system stability. From Table 3, it can be seen that in Scenario One, the total load shedding is 134.65 MW·h, while in Scenario Two, it is 98.4083 MW·h. The participation of electrolytic aluminum loads helps to reduce the losses caused by load shedding during peak electricity consumption periods.

Table 3. Analysis of wind power consumption and load shedding.

	Wind Power Consumption Volume/(MW h)	Wind Curtailment Rate/%	Load Shedding Volume/(MW h)
Scenario 1	7.8757×10^3	14.97	134.65
Scenario 2	8.0468×10^3	13.13	98.4083

4.3.3. Analysis of Load Regulation in Electrolytic Aluminum

From Figure 8, it can be seen that the electrolytic aluminum load can flexibly adjust its power consumption when wind power output reaches its peak, thereby absorbing more wind energy resources and maintaining the balance and stable operation of the power system. During peak electricity demand periods, as wind power output decreases, the electrolytic aluminum load will correspondingly reduce its power consumption to adapt to the overall demand changes in the grid, ensuring coordination between load and power supply. This dynamic adjustment mechanism not only helps to improve the absorption efficiency of wind power but also maintains system stability at different load levels, especially during peak and low electricity demand periods. The flexible response capability of the electrolytic aluminum load can effectively accommodate the fluctuations in wind power output, reducing dependence on thermal power units and enhancing the overall utilization of renewable energy.
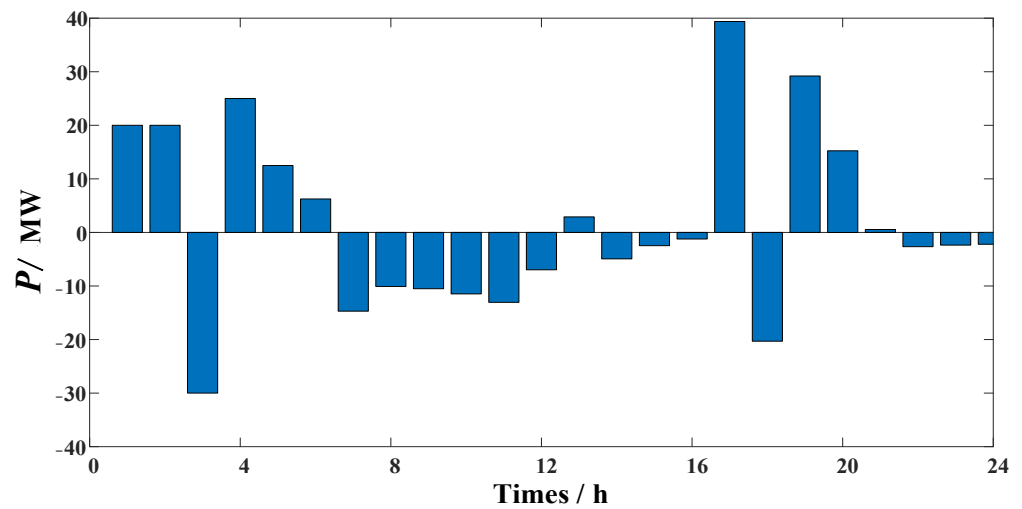
Figure 8. Aluminum electrolysis load power regulation.

Moreover, during the periods of 3:00 to 5:00 and 16:00 to 19:00, the power of the electrolytic aluminum load shows a trend of rising and then falling. This is because the power adjustment of the electrolytic aluminum load is limited by the temperature of the electrolytic cell. As the load power increases with the rise in wind power, the temperature of the electrolytic cell also increases. To ensure that aluminum production is not affected, the load power cannot remain in an upward adjustment state for an extended period. Therefore, the power of the electrolytic aluminum load also fluctuates, but the overall trend in these fluctuations is consistent with the fluctuations in wind power output, achieving the absorption of wind power.

Figure 9 illustrates the temperature variation in the electrolytic cell during the power adjustment process of the electrolytic aluminum load. When the input power of the electrolytic aluminum load increases, the temperature of the electrolytic cell also rises; conversely, when the load power decreases, the temperature of the electrolytic cell correspondingly decreases. Due to the constraints imposed by temperature changes and the associated cost variations during the adjustment process, the power of the electrolytic aluminum load cannot be adjusted indefinitely. Therefore, throughout the entire scheduling period, the temperature of the electrolytic cell fluctuates between 950 and 970 °C without exceeding the set limits, thereby minimizing its impact on the production of electrolytic aluminum load.
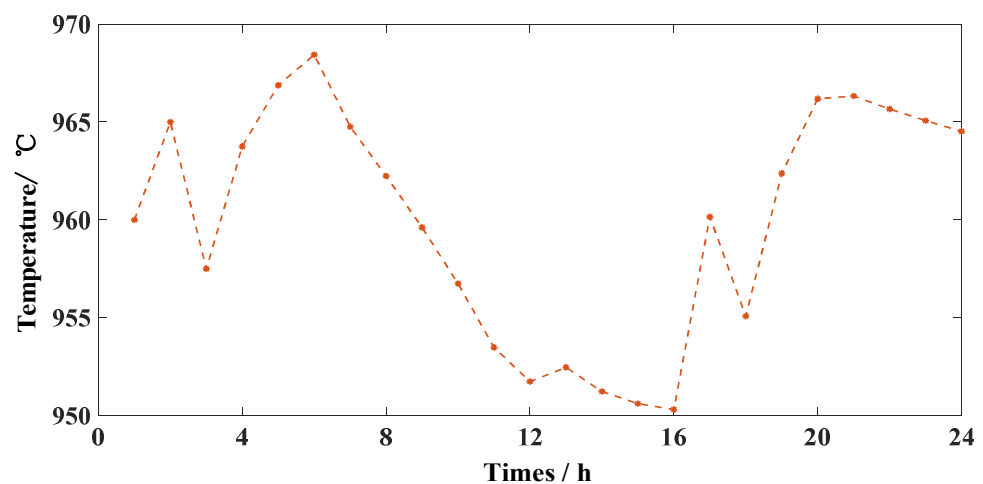

Figure 9. Electrolytic bath temperature profile.

Table 4 presents the estimated current efficiency calculated based on temperature variations during the scheduling period. It can be seen that the current efficiency was generally maintained between 93% and 95%, which did not significantly affect the normal production of electrolytic aluminum.

Table 4. Current efficiency.

	Current Efficiency/%		Current Efficiency/%		Current Efficiency/%
1	94.00	9	94.06	17	93.98
2	93.25	10	94.49	18	94.74
3	94.38	11	94.98	19	93.64
4	93.44	12	95.24	20	93.07
5	92.97	13	95.13	21	93.05
6	92.73	14	95.31	22	93.15
7	93.29	15	95.41	23	93.24
8	93.66	16	95.45	24	93.32

5. Conclusions

In this study, we propose a source-load collaborative optimization method considering the core production constraints of electrolytic aluminum loads to address key challenges in the integration of energy-intensive industrial loads and new energy power systems. Taking the temperature constraints of the electrolytic cell as the core, the impact of temperature on the chemical reaction rate, current efficiency, and production equipment life was systematically analyzed, and a coupling model between electrolytic aluminum load power regulation and core production constraints was established. Through this model, we quantified the impact of temperature changes on the production process and proposed an electrolytic aluminum load demand-side response control cost model. Furthermore, this paper constructs a day-ahead scheduling model with the optimization goal of minimizing system operating costs. Simulation results show that this method can effectively reduce the wind abandonment rate and load shedding amount of the system, and at the same time, significantly improve the system's economy and new energy consumption capacity without compromising the safety of electrolytic aluminum load production.

This study deeply combines the core production constraints of electrolytic aluminum load with power system dispatch optimization, proposes a new optimization strategy that takes into account industrial production safety and power grid operation efficiency, and fills the gap in the lack of production process constraints in high-energy-consuming load control strategies. It provides new ideas for the deep integration of power systems and industrial loads.

6. Limitations and Future Research

Although this study achieved certain results in the source-load coordinated optimization considering the core production constraints of electrolytic aluminum load, there are still some limitations.

Firstly, the control cost model in this study is based on experimental data within a specific temperature variation range, which may not fully capture the complex nonlinear behaviors in actual production processes. Future research could refine the model further by accounting for more uncertainties under dynamic production conditions.

Secondly, this study focuses primarily on day-ahead scheduling optimization, without fully considering response delays and random fluctuations in real-time scheduling. Future work could integrate intelligent control and real-time optimization algorithms to enhance adaptability to unexpected scenarios.

Additionally, the impact of market mechanisms on the regulation of electrolytic aluminum load was not fully addressed in this study. Future research could explore market incentive mechanisms to promote more effective participation of electrolytic aluminum load in grid regulation.

References

1. Xinhua News Agency. Opinions of the Central Committee of the Communist Party of China and the State Council on Completely, Accurately and Comprehensively Implementing the New Development Concept and doing a Good Job in Carbon Peak and Carbon Neutrality. 2021. Available online: https://www.gov.cn/zhengce/2021-10/24/content_5644613.htm (accessed on 23 October 2024).
2. Li, B.; Chen, M.; Zhong, H.; Ma, Z.; Liu, D.; He, G. A Review of Long-Term Planning of New Power Systems with Large Share of Renewable Energy. *Proc. CSEE* **2023**, *43*, 555–581.
3. National Energy Administration. The National Energy Administration Released the 2021 National Power Industry Statistics. 2022. Available online: http://www.nea.gov.cn/2022-01/26/c_1310441589.htm (accessed on 23 October 2024).
4. National Energy Administration. The National Energy Administration Released the 2022 National Power Industry Statistics. Available online: http://www.nea.gov.cn/2023-01/18/c_1310691509.htm (accessed on 23 October 2024).
5. Yang, H.; Liang, R.; Yuan, Y.; Chen, B.; Xiang, S.; Liu, J.; Zhao, H.; Ackom, E. Distributionally Robust Optimal Dispatch in the Power System with High Penetration of Wind Power Based on Net Load Fluctuation Data. *Appl. Energy* **2022**, *313*, 118813. [CrossRef]
6. Gerami, N.; Ghasemi, A.; Lotfi, A.; Kaigutha, L.G.; Marzband, M. Energy Consumption Modeling of Production Process for Industrial Factories in a Day Ahead Scheduling with Demand Response. *Sustain. Energy Grids Netw.* **2021**, *25*, 100420. [CrossRef]
7. Li, N. The Load Scheduling for Users Based on Demand Response and Benefit Analysis. Ph.D. Thesis, Xiangtan University, Xiangtan, China, 2016.
8. Liu, C.; Sun, A.; Wang, Y.; He, H.; Zhang, H.; Ning, L. Day-Ahead and Intra-Day Joint Economic Dispatching Method of Electric Power System Considering Combined Peak-Shaving of Fused Magnesium Load and Energy Storage. *Electr. Power Autom. Equip.* **2022**, *42*, 8–15.
9. Wu, D.; Wang, Y.; Yu, C. Demand Response Potential Evaluation Method of Industrial Users Based on Gaussian Process Regression. *Electr. Power Autom. Equip.* **2022**, *42*, 94–101.
10. Yang, N.; Xun, S.; Liang, P.; Ding, L.; Yan, J.; Xing, C.; Wang, C.; Zhang, L. Spatial-temporal Optimal Pricing for Charging Stations: A Model-Driven Approach Based on Group Price Response Behavior of EVs. *IEEE Trans. Transp. Electrif.* 2024, *in press*. [CrossRef]
11. Han, G.; Sun, R.; Xu, H.; Xu, J.; He, C.; Pi, S. Load Optimal Dispatching Modeling of Cement Industry Based on TOU Price. In Proceedings of the 2022 14th International Conference on Measuring Technology and Mechatronics Automation (ICMTMA), Changsha, China, 15–16 January 2022; pp. 772–777.
12. Li, S.; Zhang, T. The Development Scenarios and Environmental Impacts of China's Aluminum Industry: Implications of Import and Export Transition. *J. Sustain. Metall.* **2022**, *8*, 1472–1484. [CrossRef] [PubMed]
13. Chen, G.; Yang, X.; Jiang, H.; Cui, Y.; Zhang, Y.; Hao, S.; Zhang, Y. Demand Response Regulation Strategy for Power Grid Accessed with High Proportion of Renewable Energy Considering Industrial Load Characteristics. *Electr. Power Autom. Equip.* **2023**, *43*, 177–184.
14. Wang, Y.; Xie, H.; Zhu, H. Source-Load Coordinated Optimal Planning Method of Electrolytic Aluminum Industrial Park. *Electr. Power Autom. Equip.* **2024**, *44*, 132–140.
15. Yue, X.; Liao, S.; Fu, L.; Xu, J.; Ke, D.; Wang, H.; Li, L.; He, X. Hierarchical Optimization Strategy of High-penetration Wind Power System Considering Electrolytic Aluminum Energy-intensive Load Regulation and Deep Peak Shaving of Thermal Power. *Power Syst. Technol.* **2024**, *48*, 3186–3196.
16. Li, S.; Hui, H.; Bao, M. Adjustability Analysis of Aluminum Smelter Loads and Participation in Power System Scheduling. *Proc. CSU-EPSA* **2024**, *36*, 70–80.
17. Yue, X.; Liao, S.; Xu, J.; Ke, D.; Wang, H.; Yang, J.; He, X. Collaborative Optimization of Renewable Energy Power Systems Integrating Electrolytic Aluminum Load Regulation and Thermal Power Deep Peak Shaving. *Appl. Energy* **2024**, *373*, 123869. [CrossRef]
18. Yao, L.; Ding, W.; He, T.; Liu, S.; Nie, L. A Multiobjective Prediction Model with Incremental Learning Ability by Developing a Multi-Source Filter Neural Network for the Electrolytic Aluminium Process. *Appl. Intell.* **2022**, *52*, 17387–17409. [CrossRef]

19. Li, H. Research on Electrode Control Method for Aluminum Electrolysis Cell. Ph.D. Thesis, Northeastern University, Shenyang, China, 2016.

20. Wang, M. Research on Modeling and Control Method of Aluminum Electrolytic Pole Control System. Master's Thesis, Northeastern University, Shenyang, China, 2019.

21. Einarsrud, K.E.; Eick, I.; Bai, W.; Feng, Y.; Hua, J.; Witt, P.J. Towards a Coupled Multi-Scale, Multi-Physics Simulation Framework for Aluminium Electrolysis. *Appl. Math. Model.* **2017**, *44*, 3–24. [CrossRef]

22. Wong, C.-J.; Bao, J.; Skyllas-Kazacos, M.; Welch, B.; Mahmoud, M.; Arkhipov, A.; Ahli, N. Studies on Power Modulation of Aluminum Smelting Cells Based on a Discretized Mass and Thermal Dynamic Model. *Metall. Mater. Trans. B* **2023**, *54*, 562–577. [CrossRef]

23. Peng, Q. Predictive Fuzzy Control for the Temperature of Aluminium Electrolysis Process. Master's Thesis, North China University of Technology, Beijing, China, 2009.

24. Qiu, Z. *Aluminum Refining in Prebaking Tanks*, 3rd ed.; Metallurgical Industry Press: Beijing, China, 2005.

25. Ilyushin, Y.V.; Kapostey, E.I. Developing a Comprehensive Mathematical Model for Aluminium Production in a Soderberg Electrolyser. *Energies* **2023**, *16*, 6313. [CrossRef]

26. Xu, Y. A Study of Multi-Physical Fields Coupled Modelling and Structure Optimization of Large-Scale Energy-Saving Aluminum Reduction Cells. Ph.D. Thesis, Central South University, Changsha, China, 2014.

27. Yin, C. Study of Online Simulation of Thermal-Electric Field in Aluminum Reduction Cells. Master's Thesis, Central South University, Changsha, China, 2014.

28. Urata, K.; Shimizu, T. Temperature Estimation of Aluminum Electrolytic Capacitor Under Actual Circuit Operation. In Proceedings of the 2018 International Power Electronics Conference, Niigata, Japan, 20–24 May 2018; IEEE: Piscataway, NJ, USA, 2018; pp. 302–308.

29. Xu, J.; Yu, Q.; Liao, S.; Ke, D.; Sun, Y. Industrial Park Tie-Line Power Smoothing Strategy Considering Production Safety. *J. Shanghai Jiaotong Univ.* **2024**, *58*, 941–953.

30. Bao, Y. Research on Leveraging the Flexibility of Industrial Loads for Power System Frequency Operation. Ph.D. Thesis, Wuhan University, Wuhan, China, 2019.